Capabilities of monocentric objective lenses

Igor Stamenov, Ilya P. Agurok, and Joseph E. Ford

Electrical and Computer Engineering, University of California San Diego, 9500 Gilman Drive, La Jolla, California 92093-0409, USA
Author e-mail address: istameno@ucsd.edu

Abstract: Monocentric lenses (MC) enable panoramic high-resolution imaging, but have not been fully explored. We present algorithms for systematic optimization of monocentric objectives, and show the tradeoff between lens complexity and focal length, numerical aperture and spectral bandwidth.
OCIS codes: (080.3630) Lenses; (110.0110) Imaging systems; (220.3620) Lens system design.

1. Introduction

Monocentric (MC) lenses have recently changed from primarily a historic curiosity [1] to a potential solution for panoramic high-resolution imagers, where the spherical image surface is directly detected by curved image sensors or optically transferred by relay imaging or fiber coupling onto conventional flat focal planes [2-7]. MC lenses have a strong design constraint, that all the surfaces have the same center of curvature. While a small number of degrees of freedom are available (number of elements, glass selection, and radii), they can be sufficient to obtain a number of useful designs [8,9]. Nevertheless, the design space is filled with steep local minima, and it is surprisingly challenging to find near-optimal solutions for a given combination of focal length, F/# and spectral band. Rather than relying on automated lens design optimization to search for solutions, a more analytic approach is useful even if the lens geometry is as simple as symmetric two-glass ball with only three degrees of freedom [10]. To approach diffraction-limited performance as the spectral bandwidth, numerical aperture, and focal length increase, the lens must become significantly more complex, and the design space becomes harder to search. In this paper we present techniques for systematic optimization of MC lenses as a class, using analytic aberration calculations followed by constrained numerical optimization, and show the application to both fully- and hemispherically-symmetric lenses. We summarize the performance for lenses covering the visible and near IR spectral bands, and indicate trends in performance to guide lens design for a variety of MC lens based systems.

2. Monocentric lens geometries and algorithms for systematic optimization

Fig. 1 shows ten different MC lens geometries with an increasing number of degrees of freedom (DOF), meaning the total number of parameters available for optimization, bounded with a pre-defined focal length. These geometries start with the trivial: a fully symmetric glass ball with an aperture stop at the center, where given a glass choice (1 DOF), the radius is constrained by the specified focal length. They become more complex as we increase the number of glasses and radii, and break the front/back symmetry, or introduce an air gap. This list is illustrative, not comprehensive, and some of the geometries are ineffective in improving performance over less complex forms. Optimization of such "ill chosen" geometries (marked in blue) will converge to simpler forms. In general, though, the more complex forms can correct for geometric aberrations and improve lens scaling.
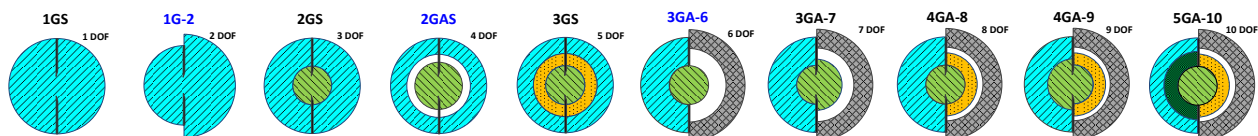

Fig. 1. Monocentric lens geometries with the increasing number of degrees of freedom.
(using naming convention **XG(A)(S)-Y** : X-number of glasses, S-symmetric, A-with an air gap, Y-where present, indicates number of DOF).

In a recently published work [10] we used a combination of Seidel 3rd order aberration analysis with exact raytrace optimization to achieve a fast global search of 2-glass symmetric (2GS) geometries for a given focal length, F-number and waveband of interest. Since the number of degrees of freedom was 3, a direct check of all 312,000 possible glass combinations (using the entire available glass catalog) yielded a one-dimensional optimization, which could be executed within minutes. Requiring a broader spectrum band and a lower F-number quickly drove the 2GS geometry to its limits, so we modified the same basic algorithm to work with a 3-glass symmetric (3GS) geometry.

In the 3GS geometry there is around 170 million glass combinations, and the optimization problem is inherently two-dimensional. In an attempt to reduce the computing time to reasonable limits, we identified and made use of an

interesting fact about 3GS geometries. In the 2-dimensional optimization space of the 3-glass symmetric system, if the glass choice is viable, areas of minimum merit function (high performance) look like a long and nearly linear ravine. So it was possible to fix the radius of second glass shell to some reasonable value, and trade the two-dimensional optimization problem for one-dimensional track along the ravine. This increased the computational efficiency and made it possible for the global search to run in 24 to 48 hours on a high performance workstation (4x2.7Hz Intel Xeon E5-4650). The freedom to choose the second radius in 3GS system was helpful in avoiding excessively thin shells solutions, which are impractical to fabricate. Unfortunately, the 3GS geometry offered only modest performance improvements, and introducing additional layers of glass did provide significant improvement. A useful solution is to break the front/rear symmetry and introducing an asymmetric air gap between the crown and flint glass core [11]. Introducing such an air gap is a common method used for control of spherochromatism [12]. This approach yields the 3 and 4-glass air gap asymmetric geometries (3GA-7, 4GA-8, and their further derivatives 4GA-9 and 5GA-10), which improve performance on extended spectral bands, larger apertures, and longer focal length systems. The four-glass with air gap (4GA-8) MC lens architecture has multiple minimums for our cost function, which is composed as the sum of the absolute values of the lateral aberrations for the tangential rays of the axial beam. The starting point for 4GA-8 systematic search is to use the core from multiple 2GS top candidates as seeds for further optimization. With the chosen glass combination we have 5 radii to optimize. These minimums are located within the nearly linear volume in the 5-dimensional optimization space, showing a linear dependence between the first and last radii. Our search for the near-global minimum begins with a gradient descent to the closest local minimum from the average radii solution for this architecture. At this local minimum the Hesse matrix and its eigenvectors are calculated. Calculations reveal two vectors with low eigenvalues. One of these vectors shows the direction of minimums group and the other shows the direction in which the cost function is very slowly increasing, but it is not clear apriori which of the two is which. We execute a number of gradient descent searches from the points uniformly located along these lines to find a global (or at least nearly global) minimum solution, and the best lens performance possible with the architecture.

3. Design results

To explore the maximum achievable performance of the MC lens geometries, we began with the design constraint of a 12mm focal length 120° FOV imager and the visible waveband of 486-656nm (specifications derived from the DARPA SCENICC program) and optimized lens design to increase aperture as much as possible subject to a pre-defined performance metric. This performance constraint was to require that the MTF was at least 70% of the diffraction limit at 200 lp/mm (the highest spatial frequency needed for Nyquist sampling of a 2.5 micron pitch sensor) while simultaneously requiring that the RMS spot size radius had to be less than 1.5x the Airy disc radius (which maintained MTF at lower spatial frequencies). While this metric is somewhat arbitrary, the trends of the results are indicative of a wide range of related performance metrics, as applied to the available degrees of freedom. The results are shown in Fig. 2a.
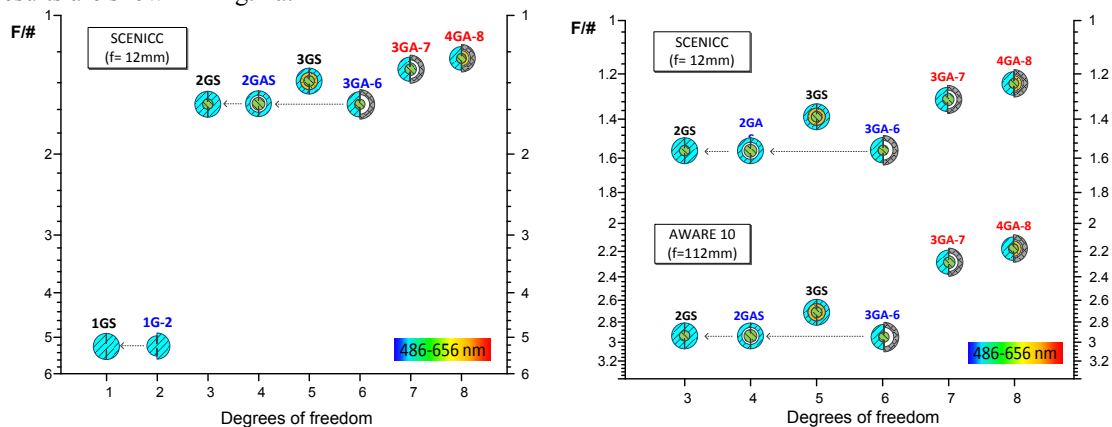

Fig. 2. Increase in lens complexity with F-number decrease on visible waveband for (a) f=12mm (b) f=12mm and 112mm comparison.

Ill chosen geometries, labeled in blue, converge to simpler ones and do not enable an increase in aperture size. The geometries labeled in black (1GS, 2GS, 3GS) show results obtained by our near-global optimization algorithm, while geometries labeled in red (3GA-7, 4GA8) are the result of the systematic 5th dimensional optimization, starting from top 2GS candidates as seed designs. Adding the second glass is helpful in controlling chromatic aberration, so there is a large increase in achievable F-number in moving from geometry 1GS to 2GS. This is

equivalent to going from a singlet lens to a cemented doublet achromat. Adding the third glass in the 3GS geometry yields apochromatic solutions on an extended waveband, whereas other degrees of freedom (specifically, 2GAS with 4 DOF, and 3GA-6 with 6 DOF) provide no improvement. The next performance increase is obtained after breaking for front/back symmetry and introducing an air gap, the 3GA-7 and 4GA-8 geometries. Similar behavior is observed when looking at the longer 112mm focal length of the AWARE10 objective lens [13], as shown in Fig. 2b.
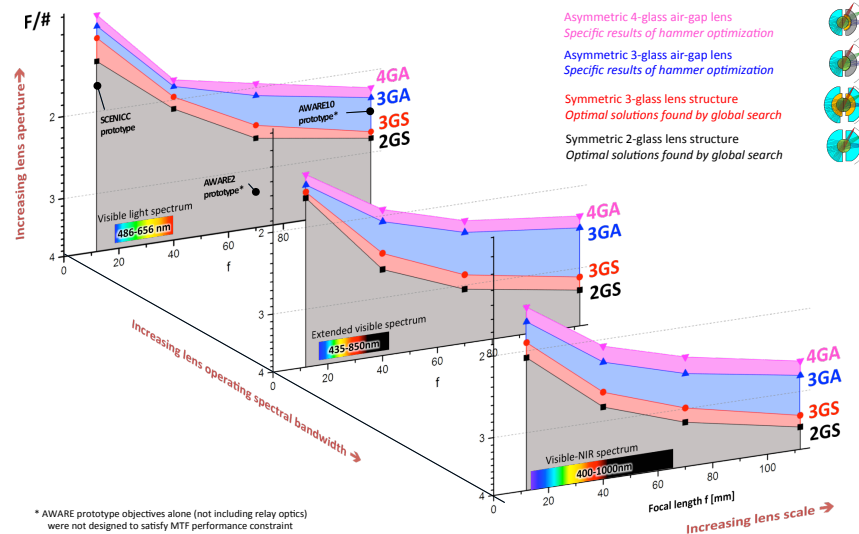

Fig. 3. Monocentric objective lens performance tradeoff for 4 different scales and 3 spectral bands (486-656nm, 435-850nm, 400-1000nm).

The final step was to explore the design space for 4 different focal lengths {12mm (SCENICC), 40mm, 70mm (AWARE2 scale [5]) and 112mm (AWARE10 scale [13])}, and at each scale look at the maximum aperture for visible, extended visible and visible-NIR spectral wavebands, subject to the MTF performance constraint described above. As before we used the near-global optimization for the 2-glass and 3-glass symmetric systems (2GS, 3GS), and for the 3- and 4-glass air gap candidates (3GA, 4GA), the combination of our systematic 5th dimensional optimizer with ZEMAX hammer optimization. The entire set of results is summarized in Fig. 3.

4. Conclusion

We observe that the simple 2-glass symmetric objective provides surprisingly good performance over a moderate waveband and scale, but the minimum achievable F/# increases with operating spectral bandwidth. However, the advantage of 4GA and 3GA over symmetric 2GS and 3GS architectures is maintained on all scales. Additionally, we note that the more complex 3GA and 4GA geometries can offer candidates with total glass weight up to 40% less than their 2GS and 3GS counterparts. In general, this class of MC objective lenses provides an extraordinary field of view, and offer the potential for a variety of wide-angle imaging systems.

5. References

[1] R. Kingslake, "A History of the Photographic Lens," (Academic, 1989), pp. 49-67.
[2] G. Krishnan and S.K. Nayar, "Towards A True Spherical Camera," SPIE Human Vision and Electronic Imaging, Jan, (2009).
[3] O. Cossairt, D. Miau, S. K. Nayar, "Gigapixel Computational Imaging," IEEE International Conf. on Computational Photography (2011).
[4] H. Son, D. L. Marks, E. J. Tremblay, J. Ford, J. Hahn, R. Stack, A. Johnson, P. McLaughlin, J. Shaw, J. Kim, and D. J. Brady, "Multiscale, wide field, gigapixel camera" in *Imaging systems Applications,* OSA Technical Digest (2011).
[5] D. J. Brady, M. E. Gehm, R. A. Stack, D. L. Marks, D. S. Kittle, D. R. Golish, E. M. Vera, and S. D. Feller, "Multiscale gigapixel photography"*,* Nature **486**, 386-389 (2012).
[6] E. Tremblay, D. Marks, D. Brady, and J. Ford, "Design and scaling of monocentric multiscale imagers"*,* Appl. Opt. **51**, 4691-4702 (2012).
[7] P. Milojkovic, J. Mait, "Space-bandwidth scaling for wide field-of-view imaging,", Applied Optics, Vol.51, Issue 4, pp. A36-A47, (2012).
[8] D.Shafer, "Some odd and interesting monocentric designs" in SPIE Proceedings 5865, 586508-586508, (2005).
[9] D. Marks, E. Tremblay, J. Ford, D. Brady, "Microcamera aperture scale in monocentric gigapixel cameras," Appl. Opt. 50, 5824-5833 (2011).
[10] I. Stamenov, I. Agurok, and J. Ford, "Optimization of two-glass monocentric lenses for compact panoramic imagers: general aberration analysis and specific designs," Appl. Opt. 51, 7648-7661 (2012).
[11] D. Marks and D. Brady, "Gigagon: A Monocentric Lens Design Imaging 40 Gigapixels," in Imag. Sys. OSA technical Digest (CD) (2010).
[12] W. Smith, "Modern Lens Design, 2nd edition", (McGraw Hill, 2005).
[13] D. L. Marks, H.S. Son, J. Kim, D. J. Brady, "Engineering a gigapixel monocentric multiscale camera". Opt. Eng. 51(8):083202